Inferring Time Variability of Stresses on Europa from Mapped Lineaments

A research proposal submitted in partial fulfillment of the requirements for advancement to Ph.D. candidacy in the Department of Geological Sciences at the University of Colorado.

Zane A. Crawford
Submitted April 17th, 2006

1. Introduction

The proposed study investigates possible temporal and spatial variation of stresses in the ice shell of Europa by correlating mapped lineaments with stresses induced by diurnal and longer period tides. Stresses are calculated using a model based on the gravitational potential with a viscoelastic ice shell (Wahr et al. in preparation). The study hopes to discern the most likely stress environment in which the lineaments formed, how the physical properties of the ice shell have evolved with time, and whether surface activity is continuous or episodic, thus addressing basic questions about Europa's geological history, and whether there is the potential for a continuously or episodically available energy supply capable of sustaining a subsurface biosphere.

1.1 Setting/Background

Of the major satellites in the Jovian system Europa is the smallest, being approximately the same size as Earth's own moon. It is frequently referred to as an 'icy' moon, but with a density of 3.01 g/cm^3 it is actually a mostly rocky body, with only a thin veneer of H_2O covering its surface (Greeley et al., 2004). Despite its small size, Europa has a nearly craterless surface, with an inferred age of tens to hundreds of millions of years (Zahnle et al., 2003), covered with linear features believed to be related to fracture and faulting of the icy shell (Greeley et al., 2004). Radiogenic heating alone is insufficient to maintain activity in a body the size of Europa for the age of solar system, and so another energy source must be invoked to drive the moon's activity. Europa's slightly larger sibling Io is virtually seething with volcanism due to dissipation of tidal energy in its interior, which leads to partial melting of its silicate mantle (McEwen et al., 2004). Like Io, deep within the Jovian gravity well, Europa is forced into an eccentric orbit by its resonance with neighboring moons, and must also be dissipating tidal energy internally. Although it is unclear whether this tidal dissipation is taking place within the icy shell, within the silicate mantle, or both, it is ultimately thought to be the primary source of the energy that drives resurfacing (Cassen et al., 1982).

Additionally, there is evidence that beneath Europa's icy surface there lurks a deep, salty, liquid water ocean. The Galileo magnetometer detected an induced magnetic field in Europa's vicinity, consistent with a global, spherical, conducting layer beneath the ice. The most plausible explanation of such a global conducting layer seems to be a salty ocean (Kivelson et al., 2000). Such a global ocean, if it decouples the motion of the ice shell from the rocky interior, has important implications for the stresses which the ice shell experiences.

Europa's rotation and position within Jupiter's gravitational potential causes the moon to take on a tri-axial ellipsoidal figure, prolate about the Europa-Jupiter axis, and oblate about its rotational axis. Because of its forced eccentric orbit (e = 0.01), over the course of its 85 hour day Europa experiences changes in the gradient of the gravitational potential – tides – as it moves toward and away from Jupiter. When it is close in, the moon is forced to take on a more prolate shape – it is stretched out along the line connecting it to Jupiter. As it moves further away, and up out of the gravity well, the gradient of the gravitational potential becomes smaller, and the moon is able to take on a slightly more spherical shape.

Europa also experiences a diurnal *librational* tide. Because the moon is constrained to rotate at a constant rate, but the rate at which it orbits Jupiter varies according to Kepler's 3rd law, the permanent tidal bulge is sometimes leading and sometimes trailing Jupiter's position, always facing the empty focus of Europa's elliptical orbit, nodding back and forth once each orbit by 2e (twice the orbital eccentricity), see Fig. 1.1. The combination of the radial and librational tides results in an unusual pattern of time-variable stresses on the surface. Previous work has shown that the enigmatic cycloidal ridges on Europa can be explained, at least in part, by the these diurnal stresses (Hoppa, 1998; Hoppa et al., 1999). If the ice shell is underlain by an inviscid, hydrostatic layer (the ocean), which decouples it from the rocky interior, the diurnal tides ought to have a maximum amplitude of ~30 m. Without a decoupling fluid layer, the diurnal tides are

expected to be only ~1 m high (Moore and Schubert, 2000). A 1 m tide is unlikely to generate enough stress to fracture the ice, and so the cycloidal ridges are considered further evidence of a subsurface ocean.

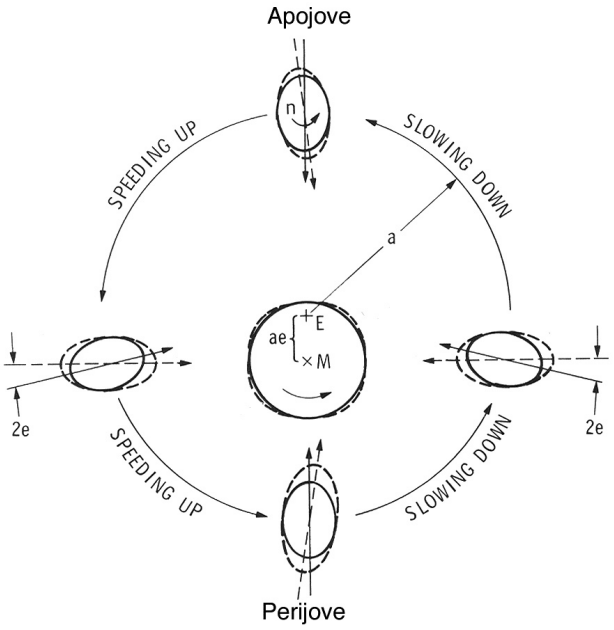

Figure 1.1: Schematic showing Europa's libration as it orbits Jupiter. Dashed ellipse shows the orientation of the potential minimum, solid ellipse shows the actual orientation as required by a constant rotation rate (after Yoder).

Another consequence of Europa's eccentric orbit is that the ice shell may experience a net torque over the course of an orbit. If it is also decoupled from the interior by a global ocean and free from significant mass anomalies, the shell would be expected to rotate at a slightly faster than synchronous rate. The rate of this hypothesized rotation has been estimated to be on the same order as the thermal diffusion timescale of the ice shell, 10^7 years (Ojakangas and Stevenson, 1989a). The rotation rate has been observationally constrained to be slower than one rotation every 10^4 years by comparing the positions of features in Voyager and Galileo images (Hoppa et al., 1999)

If the ice shell is rotating non-synchronously, the stresses that it experiences as a result will depend on the ratio of the rotation period to the shell's Maxwell (viscous relaxation) timescale, as the two rates compete – rotation causes a build up of stress, and viscous relaxation reduces stress. The rate of NSR and the amount of stress which is relieved viscously may change with time if the properties of the ice shell vary – for example if the proportion of tidal energy dissipated in the ice shell vs. the silicate mantle changes as the strain in the ice (and thus its viscosity) change, or if the overall thickness of the ice shell varies as a result of the onset or cessation of solid state convection. Previous work has shown that the patterns of many of the global scale lineaments on Europa are consistent with formation as tensile fractures due to NSR of the ice shell (Helfenstein and Parmentier, 1985; McEwen, 1986; Leith and McKinnon, 1996; Greenberg et al., 1998; Geissler et al., 1998), indicating that for at least some periods of time, viscous relaxation is probably unable to completely relieve the stresses built up in the shell through NSR.

Interestingly, the formation of cycloidal lineaments due to diurnal tides, and global lineaments due to NSR of the ice shell are to some degree mutually exclusive. If NSR stresses are dominant, they should swamp the diurnal variability which is necessary to create cycloids, and if diurnal stresses are dominant, it is not clear how features consistent with NSR stress patterns are formed. There are also many lineaments both small and large that have "wavy" shapes somewhere between linear and cycloidal. Thus, it appears that a continuum of stress regimes are recorded on Europa's surface.

Previous work has shown that feedback among internal structure, dissipation of tidal energy, and orbital dynamics is potentially important in the Io-Europa-Ganymede system (Showman and Malhotra, 1997; Hussman and Spohn, 2004). Changes in Europa's heat flow could result in the initiation or cessation of solid state convection in the ice shell, or a shift in tidal dissipation between the moon's icy shell and silicate mantle. Changes in heat flow would also be important in determining the availability of chemical energy in the subsurface ocean, and thus Europa's habitability over time. These same changes in internal processes can affect the stresses in the ice shell, and thus a record of them may be observable in the lineaments on the surface. The present study proposes to use several techniques to extract information from the lineaments about the temporal variation of stresses on Europa's surface.

1.2 Determining Relative Ages of Surface Regions on Europa

On most planetary surfaces, crater counts are used to determine the relative and in some cases absolute ages of features. However, because the surface of Europa appears so young, the population of secondary craters may dominate the cratering population, making determining relative ages difficult (Bierhaus et al., 2001). Absolute ages are even more elusive (Zahnle et al., 2003). Fortunately, there

are several potential ways of assessing the relative ages of features on Europa that make use of the lineaments themselves.

First, if it is assumed that the shell has undergone non-synchronous rotation, and one looks at those global lineaments which broadly appear to fit the NSR stress pattern when translated longitudinally by some amount, we can use the amount of translation as a proxy for relative age. Those lineaments which require more back-rotation to match the expected pattern of failure must have formed longer ago. This technique can only create a unique order of formation under the assumption that all of the global lineaments formed within a single rotation of the ice shell. This seems a reasonable assumption, given that a large majority of the global lineaments are consistent with NSR stresses from a ~60° range of shell orientations.

Second, in medium to high resolution images of Europa's surface, intersecting lineaments commonly have well defined cross-cutting relationships. Any time two features intersect, and one is clearly on top of the other, information is available about their relative times of formation or last activity. The densely interconnected nature of the lineaments on Europa makes this a potentially rich source of information about the time-evolution of the stresses.

Third, the shapes of the cycloidal features, which are believed to result from stresses induced by the diurnal tides, are sensitive to a variety of parameters, including their location of formation, the amount of NSR stresses present in the shell, the Love numbers describing the internal distribution of mass within Europa, and a variety of material properties of the ice (Hoppa et al., 1999). While the relative rarity of cycloidal features makes it difficult to work them into a global stratigraphy based on cross cutting relationships, determining the stress environments most likely to have resulted in their formation may yield useful constraints applicable to the other two techniques listed above.

1.3 Necessary Components and Capabilities

To make use of these potential sources of information about the temporal variation of stresses on Europa requires us to bring together several tools and techniques.

We will need to develop a physical model of the stresses that result from tides. The model should allow us treat Europa as the complex, differentiated body it is, with a silicate interior and liquid water ocean, in addition to the two layer ice shell. The model should treat the ice shell as a viscoelastic solid, with a cold brittle upper layer, and a warm ductile lower layer. It should be able to separate the stresses due to diurnal tides and NSR. It needs to allow us to vary the rate of NSR and the viscoelastic properties of the ice. Because the two sources of stress which we are considering act on very different timescales (85 hours vs. $>10^4$ years), the model will also need to allow us to use different frequency-dependent parameters for NSR and diurnal stresses. Ultimately we will need to benchmark the model against previously published work, and account for any differences.

We must also have the ability to make quantitative comparisons between our modeled stresses and mapped lineaments. We can make these comparisons either by synthesizing lineaments based on the calculated stresses, and comparing their shape to the shape of the corresponding mapped lineaments, or by comparing the expected direction of failure to the observed orientation of each small line segment making up a mapped lineament, and adding up the errors accumulated along a lineament's entire length. The first technique will be more useful when looking at lineaments forming in a time variable field (e.g. the cycloids), and the latter will be more useful when trying to compare a large set of lineaments to a particular field, which is not variable (e.g. finding the single best fit between NSR stresses and the entire set of global lineaments). For features like the cycloids, whose shapes depend on many input parameters, we will need to develop an automated method of searching parameter space to find the set which provides the best fit, within certain bounds.

In order to be able to distill scientifically useful information out of the many individual superposition relationships which we will map in medium and high resolution images, we will need to develop an algorithmic approach, which allows a computer to assist us in sorting out the many temporal relationships. Since the network of intersecting lineaments is unlikely to provide enough information to completely constrain their order of formation, it will be important to design an algorithm which allows us to quantify the uncertainty of any feature's relative time of formation. The technique will need to be validated against many synthetic datasets of lineaments with a variety of known formation histories.

1.4 NASA Objectives Addressed by the Proposal

The present proposal is most relevant to Sub-goal 3C of the 2006 NASA Strategic Plan: "Advance scientific knowledge of the origin and history of the solar system, [and] the potential for life elsewhere…"

It also addresses several portions of the Outer Planets Research program, including: "Enhancing the scientific return from the Galileo [and] Voyager

… missions by broadening scientific participation in the analysis of their respective data sets," "Improving our understanding of the … evolution of the outer Solar System, including the giant planets [and] their satellites…," and "Development of basic theory… and modeling relevant to the interpretation of mission data…."

2. Modeling Tidal Stresses on Europa

Previous models of Europa's stresses have made simplifying assumptions about the moon's internal structure, and have treated the icy shell as a purely elastic solid (Greenberg et al., 1998; Hoppa, 1998). I will calculate Europa's stresses using the gravitational potential model of Wahr et al. (in preparation), which treats the satellite's shell as a viscoelastic Maxwell solid.

2.1 The Viscoelastic Stress Model

Our research group has developed a model based on the gravitational potential in the vicinity of Europa. The model uses the degree two Love numbers h_2 and l_2 calculated based on a realistic interior, depicted in Fig. 2.1, composed of a silicate core, liquid water ocean, and two layer viscoelastic ice shell, allowing for different viscosities in the cold upper (brittle) and warm lower (ductile) portions of the icy shell (Mullen, 2006; Wahr et al., in preparation).

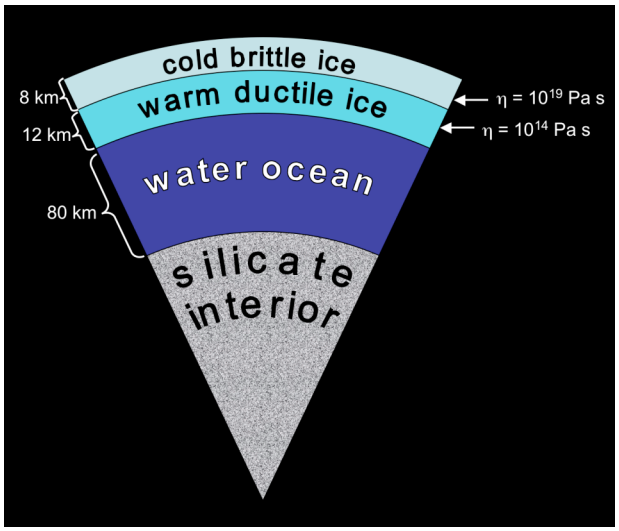

Figure 2.1: Interior structure of Europa used to calculate the degree 2 Love numbers h_2 and l_2. Layer thicknesses and viscosities are nominal values.

Given the gravitational potential and the Love numbers, I can calculate the displacement vectors, strain and stress tensors for an arbitrary point on the surface, at any point in the orbit. When diagonalized, the stress tensor yields the principal horizontal components of the stress field. The model is capable of calculating purely diurnal stresses (in which the NSR rate is zero), and purely NSR stresses (in which the orbital eccentricity is artificially set to zero), as well as any combination of the two. The model is also capable of treating the entire ice shell essentially elastically (if the viscosities of both layers of the ice shell are made very large), which will be useful for comparison to previously published results.

In order to treat the ice shell viscoelastically, frequency dependent (complex) Love numbers and Lamé parameters must be introduced. Because diurnal and non-synchronous stresses have very different forcing frequencies, the stresses from these two mechanisms must be calculated using two different sets of Love numbers and Lamé parameters. There are three general stress regimes which the shell may inhabit, depending on the relationship of the NSR forcing period, ω_{NSR}, to the Maxwell (viscous relaxation) timescales of the upper (cold) and lower (warm) layers of the ice shell, τ_u and τ_l respectively:

1.) $\omega_{NSR} < \tau_l < \tau_u$: The entire shell behaves elastically in response to NSR, allowing significant NSR stresses to build up, potentially leading to fracturing indicative of NSR.

2.) $\tau_l < \omega_{NSR} < \tau_u$: The lower shell behaves viscously in response to NSR, and does not support significant stresses, but the upper ice shell responds elastically, effectively concentrating NSR stresses in the upper portion of the shell, again potentially leading to fractures indicative of NSR.

3.) $\tau_l < \tau_u < \omega_{NSR}$: The entire shell behaves viscously in response to NSR, preventing significant NSR stresses from building up, leaving diurnal stresses to dominate fracturing of the surface.

Previously, using an elastic model, the interplay between ice viscosity and shell rotation rate has been encapsulated indirectly by specifying a particular amount by which the permanent bulge is displaced from the sub-Jovian point. For example, "5° of NSR stresses" meant that the bulge was displaced by 5° from the equilibrium point. In the viscoelastic model, this parameter is no longer needed. Instead, the ice shell viscosities, and the NSR forcing frequency are specified directly. For a given viscosity, a higher forcing frequency results in greater stresses, and vice versa.

2.3 Benchmarking the Model

For the NSR stresses the model in elastic mode (using frequency independent Love numbers and Lamé parameters) can be compared to an implementation of the "method of flattening" first described by Melosh (1977) and subsequently used by others (Helfenstein and Parmentier, 1985; Leith and McKinnon, 1996; Greenberg et al., 1996; Hoppa, 1998). The match is exceptionally good, with the principal components of the stresses having exactly the same orientations, and for an appropriate choice of love numbers (h_2/l_2 = 4) at worst a 2% difference in stress magnitude in regions where stresses are significant (Note that in transitional areas where the stresses are small, the percentage difference between the two models can be large, but the absolute difference in magnitude is very small, ~10s of Pa).

For the diurnal stresses, I do not have an implementation of a previous model to check our results against, and the published plots lack sufficient resolution for a meaningful comparison. However, Hoppa et al. (1999) published modeled reproductions of several cycloidal ridges based on the diurnal stresses, and the associated parameters which were used to fit their shapes – crack propagation speed, ice strength, longitude of formation, etc. If the viscoelastic stress model is reproducing the earlier elastic diurnal stress model, I will be able verify it by reproducing his cycloidal forms with the same input parameters. To date however, my modeled cycloids have somewhat different paths than Hoppa's, and I am working to understand this discrepancy.

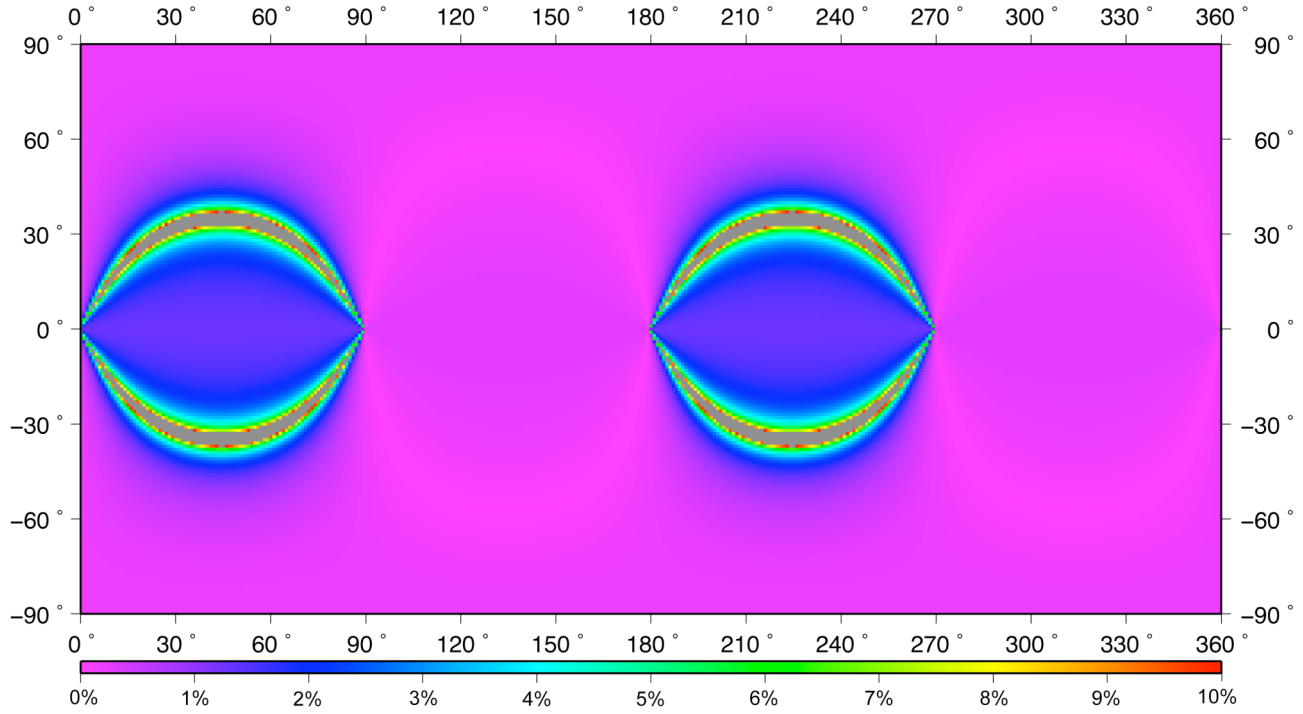

Figure 2.2: Ratio of the magnitude of the vector difference between the greatest tensile stress as calculated by Melosh's method of flattening and Wahr's gravitational potential method, to the magnitude of the greatest tensile stress as calculated using the method of flattening. Arcuate regions of large percentage differences are due to the small absolute magnitudes of the stresses in those areas. Plot is identical for greatest compressive stresses, but shifted by 90° in longitude.

3. Comparing Global Lineaments to NSR Stresses

One of the simplest analyses which this stress model allows is the comparison of large scale lineaments to the static stress field that results from non-synchronous rotation of the icy shell. This kind of analysis has been performed for global-scale lineaments in aggregate (Helfenstein et al., 1985; Leith and McKinnon, 1996; Greenberg et al., 1998; Geissler et al., 1998). Our stress model and digital mapping techniques (discussed next) allow me to easily make the comparison quantitatively on a lineament by lineament basis, allowing me to build up a histogram showing the amount of "global" lineaments formed versus the amount of ice shell back rotation, and may indicate whether global lineaments have formed continuously or

episodically. If lineaments have formed episodically, then either the magnitude of NSR stress has been changing with time, or the mechanism of relieving NSR stress has changed with time.

3.1 Mapping the Global Lineaments

Before any comparison can be made to the modeled stresses, I need to map those features that are of interest. It is important to ensure that the study is not biased in its selection of lineaments for comparison due to the uneven data coverage we have for Europa. Only a relatively small portion of the surface has been imaged at regional scale or higher resolution, and it will be easier to pick out individual lineaments for comparison in those areas. To avoid this bias, the global map can be re-sampled at a resolution which simulates even coverage of the majority of the surface (between 0.9 and 2 km per pixel). From such a map all arcuate features which exceed a certain minimum length may be mapped in GIS. Then, using the technique described below, I will select for analysis only those features which, for some amount of shell back rotation, have a maximum misfit to the NSR stress field below a chosen threshold. This way the metrics used for selection are quantified: the resolution per pixel of the re-sampled map, the minimum length, and the maximum misfit allowed between the lineaments and the NSR stresses. Thus I will be able to test the sensitivity of my results to each of these parameters.

3.2 Comparing Mapped Lineaments to a Static Stress Field

To compare a mapped lineament to a static (e.g. NSR) stress field, I adopt the following procedure:

1.) For each line segment making up a lineament, calculate the principal components of the stresses at the midpoint of the segment.
2.) If the line segment is so long as to make a single calculation at its midpoint unrepresentative of the stresses along its entire length, break it into smaller segments, or ignore its contribution to the overall error.
3.) Calculate the expected orientation of failure. In regions where at least one principal horizontal stress is tensile, this is perpendicular to the greatest tensile stress. In regions of biaxially compressive horizontal principal stresses, this should be approximately ±30° from the direction of greatest compressive stress.
4.) The difference between the orientation of the observed (mapped) lineament segment, and the expected direction of failure is the "error" for that segment.
5.) Calculate the root mean square (RMS) error of an entire lineament by taking the square root of the sum the squares, and dividing it by the number of lineament segments.
6.) Error contributions should be weighted linearly according to the lengths of the segments from which they come (i.e. the error from a segment 20 km long should count for twice as much as the error from a segment 10 km long)

It may also be necessary to introduce weighting factors dependent on the magnitudes of the stresses (if disagreement in a region with lower stresses are deemed less important), or on how isotropic the stresses are (since when the stresses are nearly isotropic, it only takes only a very small perturbation to change the orientation of the principal components). However, such weights would introduce more subjective judgement.

Comparisons between stresses and lineaments in areas where tensile failure is expected are more straightforward than in regions of compressive stresses. It may be useful in compressive regions to construct a histogram for each lineament showing the distribution of misalignment between observed and predicted direction of failure. If a strong bimodal distribution of errors is found to be centered on the orientation of the most compressive principal stress, that is a good indication of compressive failure. However, since much of the ice shell experiences tensile stresses, and most materials are significantly weaker in tensile failure than compressive/shear failure, we will initially focus primarily on modeling the fractures as due to tensile failure (Leith and McKinnon, 1996).

3.3 Preliminary Results Comparing NSR Stress to Global Lineaments

I have successfully used this method of comparison to reproduce previously published results for fits between the NSR stresses and the global lineaments in aggregate, finding a best fit between the set of all global scale lineaments which qualitatively appear to match the NSR stress field in tensile failure, at 33° of shell back rotation (Crawford and Pappalardo, 2006). See Figs. 3.1, 3.2a and 3.2b below. This is slightly greater than the ~25° of back rotation inferred by McEwen (1986) and confirmed by Leith and McKinnon (1996), which is consistent with Galileo imaging identifying some additional global lineaments beyond those imaged by Voyager (Geissler et al., 1998)

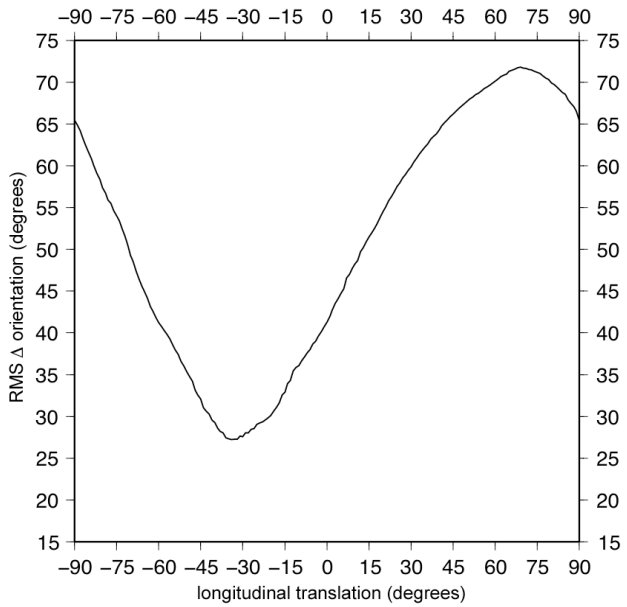

Figure 3.1: RMS difference in orientation between the set global lineaments (as shown below in Fig. 3.2) and the expected orientation of tensile failure in a purely NSR stress field (also as shown in Fig 3.2), for various amounts of east positive longitudinal translation. Best fit is at 33° west of their current locations.

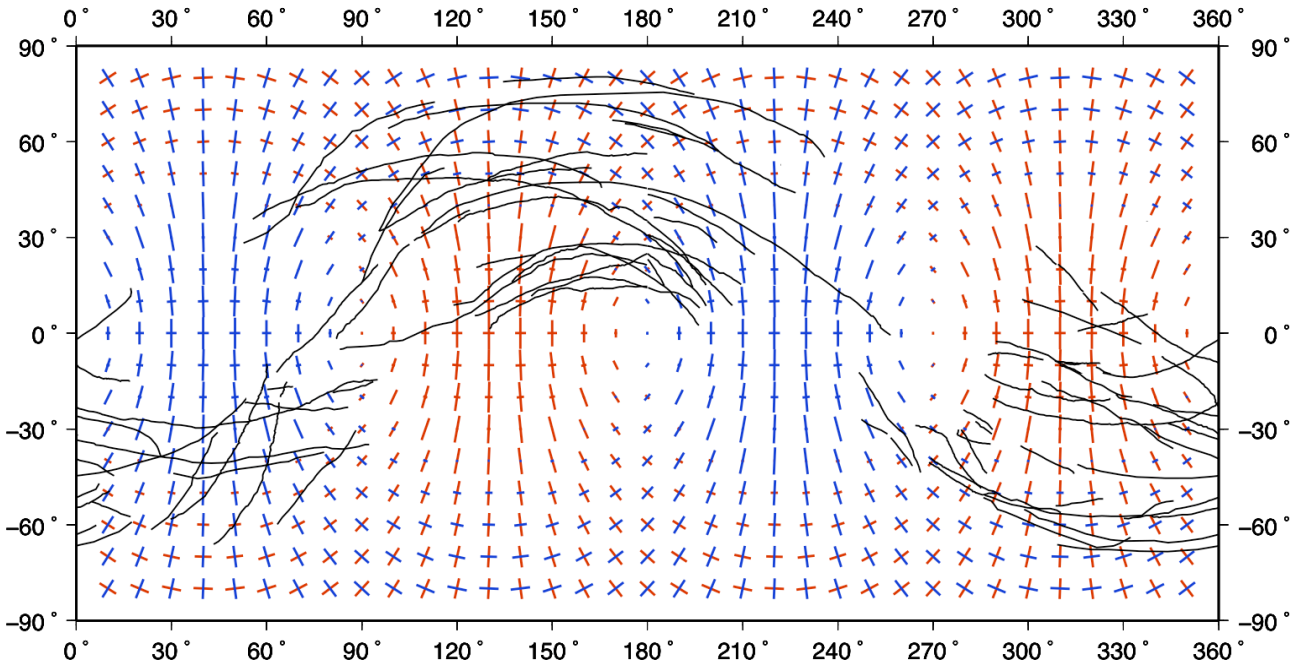

Figure 3.2a: Global lineaments (black) as mapped, superimposed upon the pattern of principal stresses due to NSR as calculated using a one-layer elastic ice shell with the permanent bulge displaced by 5°. Red indicates tensile stresses, blue indicates compressive stresses. Tic length is proportional to magnitude.

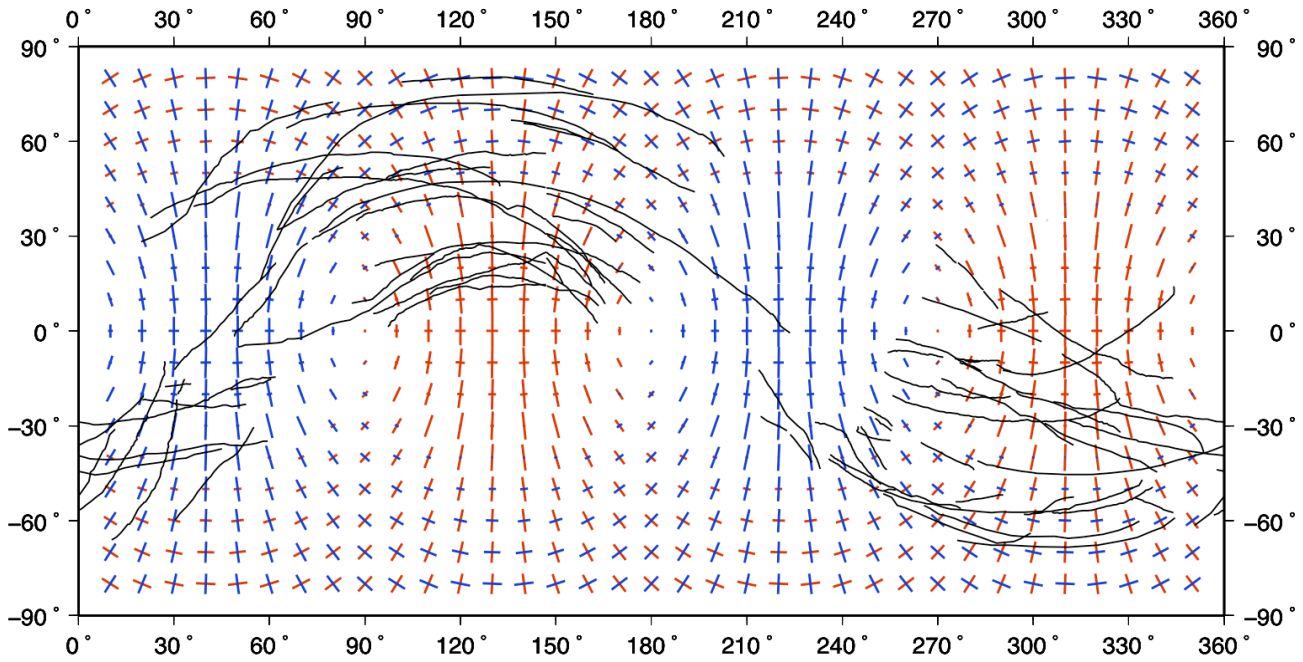

Figure 3.2b: As in Fig. 3.1a, but with the global lineaments shifted 33° to the west, corresponding to their best aggregate fit to the tensile stresses due to NSR of the ice shell.

4. Quantitatively Comparing Synthetic and Mapped Lineaments

There are many circumstances where it will be useful to create synthetic lineaments based on calculations from our model, including:

1.) To test the sensitivity of lineament morphology to various input parameters;
2.) To synthesize *particular* mapped lineaments in order to learn about the stress environment in which they formed; and
3.) To create synthetic sets of cross-cutting lineaments with *known* histories to test how effective the stratigraphic sorting technique (described below) is at reconstructing lineament order of formation, time variability of stress fields, and lineament re-activation.

Next I will discuss methods for generating synthetic lineaments.

4.1 Synthesizing Lineaments in a Static Stress Field

In a static stress field such as that from NSR, a starting location on the surface of the satellite is chosen, the principal components of the stresses are calculated there, and a fracture trajectory is calculated based on the stress field. In tensile failure, this trajectory will be perpendicular to the greatest tensile stress. The crack is incrementally propagated a predetermined distance in the direction of failure along spherical geodesics, and the process is repeated at the new location, with each location sequentially output to a file defining the shape of the lineament. The lineament is allowed to propagate until it either reaches a predetermined maximum length, or until it enters a region where the stresses no longer exceed the presumed tensile strength of the ice. For a static stress field, it is easy to allow the lineament to propagate both eastward and westward simultaneously.

4.2 Synthesizing Lineaments in Dynamic Stress Fields

One can also imagine a fracture propagating across the surface of Europa on the timescale of a Europan day, allowing the stresses controlling the propagation to vary both with location and time. Depending on the material properties of the ice and the sources of stress which are included in the simulation, such fractures may propagate continuously over the entire orbit, or they may be active for only a portion of the day. Hoppa et al. (1999) first demonstrated that fractures which experience significant cyclical changes in their trajectory due to the varying diurnal stresses, and which are only active for a portion of each orbit may

resemble the enigmatic cycloidal lineaments.

Lineaments formed in a stress field which is a combination of the static NSR field and the dynamic diurnal field can have generally sinusoidal shapes in a continuum from sharp-cusped cycloids (when diurnal stresses dominate) to arcuate (when NSR stresses dominate), mimicking the variation we see in the forms of lineaments on Europa's surface.

As with the synthesis of lineaments in a static field, creating lineaments in a time varying field is an iterative process, the main difference being that a consistent sense of time must be incorporated. The fractures can still be allowed to propagate a certain fixed distance between successive iterations, but we must calculate the corresponding increment in time or orbital position, so that we know what inputs to give the next stress calculation, based on the average speed at which the crack is propagating.

4.3 Exploring the Morphology of Sinuous Lineaments

With a system for simulating the formation of lineaments in a time-variable stress field, the influence of each input parameter on the morphology of the lineaments can be examined. In order to do these comparisons quantitatively, some way is needed of measuring how different two linear shapes are from each other. Despite the fact that the shapes which are being compared are one dimensional in a two dimensional (lat/lon) space, a conventional fitting method cannot be used because neither of the spatial axes are independent. Additionally, the two dimensional physical space we are working in is actually the surface of a sphere.

To facilitate the comparison between two arbitrary linear shapes, I use a concept from metric geometry: the mean Hausdorff distance or MHD (e.g. Gromov, 1999). Frequently utilized in machine vision for comparing complex shapes, the MHD is defined as follows: for two linear shapes A and B, each composed of a finite number of individual points, the MHD from A to B is defined as the sum of the distances from each point in A to its nearest neighbor in B, divided by the number of points in A. ("Distance" in this context can be defined as any function of the coordinates defining the points being compared in A and B. We use the spherical geodesic.) It is important to note that MHD(A,B) is in general not equal to MHD(B,A). This can lead to degenerate comparisons, in which two dissimilar shapes have a small MHD, e.g. the MHD from a short line segment which coincides with a small portion of a larger, more complex linear feature will be very small. I define a new quantity, the symmetric mean Hausdorff distance (SMHD) such that:

$$SMHD = [MHD(A,B) + MHD(B,A)] / 2$$

which has a unique minimum when the two shapes being compared are identical.

The relative importance of any input parameter X to the generated lineament's form can be determined in units of $\Delta SMHD/\Delta X$. The dependence is only likely to be close to linear for explorations of any small neighborhood within parameter space, but with a large number of samples, it should be possible to map out the relative importance of the different inputs, as well as the variability in importance for any particular input. Parameters to explore, and their qualitative influences on lineament morphology include:

- **Location of formation**: Influences the overall trajectory of the crack, especially in the presence of significant NSR stresses.
- **Direction of crack propagation**: Determines what region of the stress field the crack propagates through, and also the orientation of the cusps in cycloidal features.
- **Ice strength**: Determines for what portion of an orbit a fracture is active, and so influences how long individual segments of cycloidal lineaments are. Determines the ultimate self-termination location.
- **Crack propagation speed**: Influences the "wavelength" of sinuous variations within lineaments.
- **Orbital eccentricity**: Determines the magnitude of variations due to diurnal stresses, and ultimately the net torque on the ice shell.
- **Love numbers (internal structure)**: Subtle but pervasive effects on overall lineament morphology and trend.
- **Viscosities of the ice shell**: Changes the relaxation time, in part determining how much NSR stress can actually be stored in the ice shell. Controls the effective elastic thickness of the shell, influencing the Love numbers.
- **Forcing timescale (rotation period) for NSR**: With inverse effects to those of viscosity, determines how much stress can be relaxed away viscously.

4.4 Reproducing Cycloidal and Sinuous Features

Beyond simply testing the sensitivity of lineament morphology to input parameters, I can also attempt to reproduce individual mapped lineaments in order to place constraints on the parameters which determined the stress

environment in which they formed. The parameter space to be searched is so large that it is impossible to exhaustively explore it. Instead a directed search method is needed to find those portions of parameter space which are best able to reproduce the lineaments of interest. The simplest approach is trial and error, generating lineament after lineament, keeping in mind the qualitative effects of each parameter as listed above. While this does allow one to do a decent job of reproducing lineaments, it is easy to get stuck searching a particular portion of parameter space that seems to work well, while ignoring others that may work equally well or better.

To avoid this problem I adopt the neighborhood algorithm (NA) with a Gibbs sampler, as described in Sambridge (1999a). This parameter space search method is computationally efficient, and dynamically adapts to the search space, preferentially sampling any areas which are found to do a good job of reproducing the objective function. It also results in a large ensemble of samples from all over parameter space, which can be statistically analyzed to yield generalizations about the model and objective functions (Sambridge, 1999b). In this case, the distance between the model and objective function corresponds to the SMHD between a generated lineament and the mapped lineament it seeks to reproduce.

Using this kind of directed search, and modeling the ice shell purely elastically, I have been able to reproduce the mapped cycloidal lineaments that occur at high latitudes, with best fit SMHD values of less than 10 km, meaning that the average distance between a point on the mapped lineament and the nearest point on the synthetic lineament is less than 10 km. I am thus far unable to reproduce cycloidal lineaments which occur at low latitudes, and to my knowledge no other workers have been able to reproduce them either. This suggests that either some other process is responsible for the cycloidal lineaments, or that they may have formed when the ice shell was in some other orientation, suggesting true polar wander of a floating ice shell (Ojakangas and Stevenson, 1989b; Leith and McKinnon, 1996; Sarid et al., 2002). If polar wander were to occur on a timescale significantly greater than the viscous relaxation time of the ice shell, lineaments could be arbitrarily translated and rotated on Europa's surface without ever displaying morphology indicative of polar wander stresses. I will improve our directed search method to include arbitrary translation and rotation of lineaments in spherical coordinates to test whether the morphologies of the low latitude cycloidal lineaments are consistent with some combination of diurnal and NSR stresses when true polar wander is allowed.

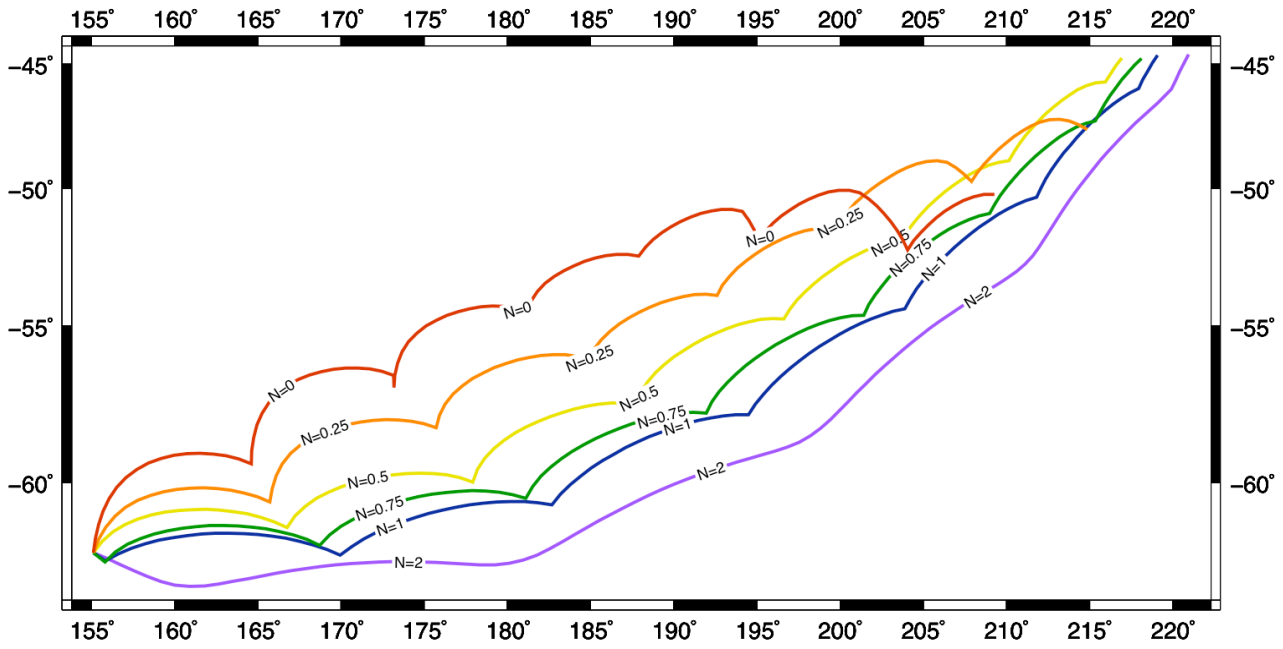

Figure 4.1a: Variation in planform of a synthetic Cilicia Flexus (see Fig. 4.2b), with increasing contributions to the stress field from NSR. The irregular red lineament is due to purely diurnal stresses (NSR=0°). The purple "wavy" lineament is active throughout the entire orbit (with NSR=2°).

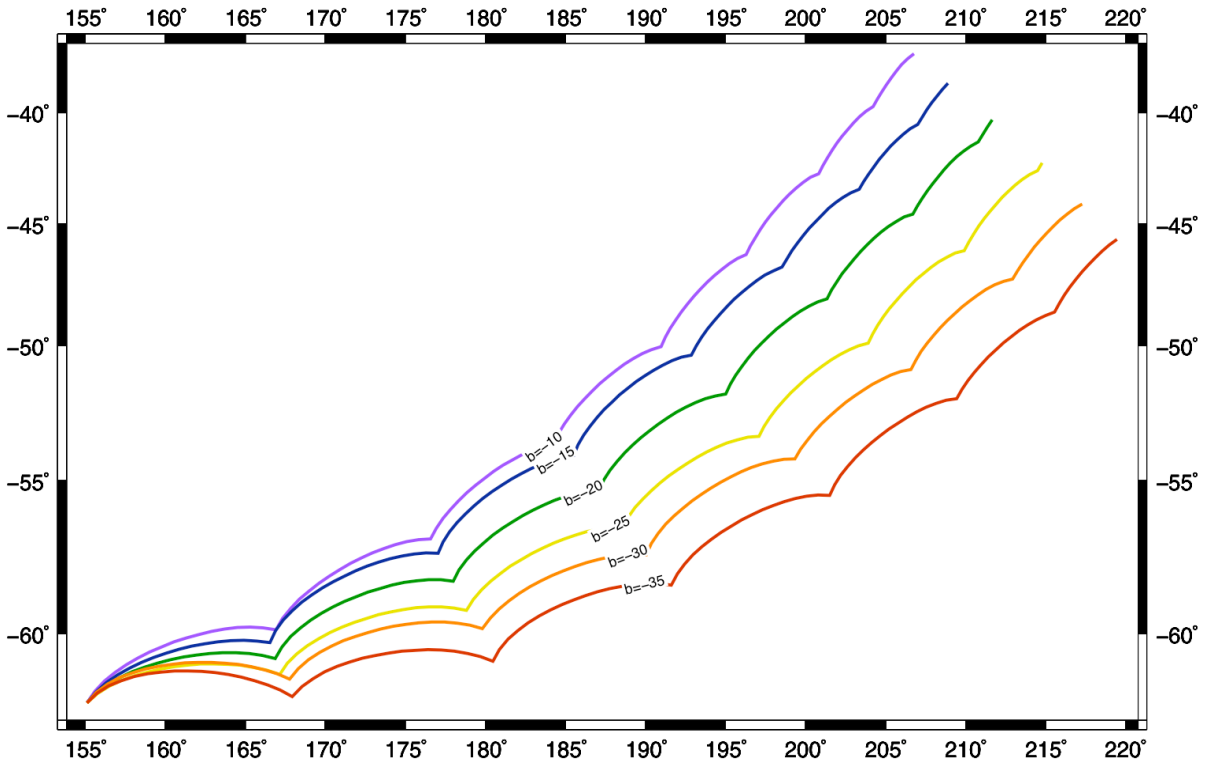

Figure 4.1b: Variation in the planform of synthetic Cilicia Flexus with different longitudes of formation. b = east positive longitude shift from mapped location.

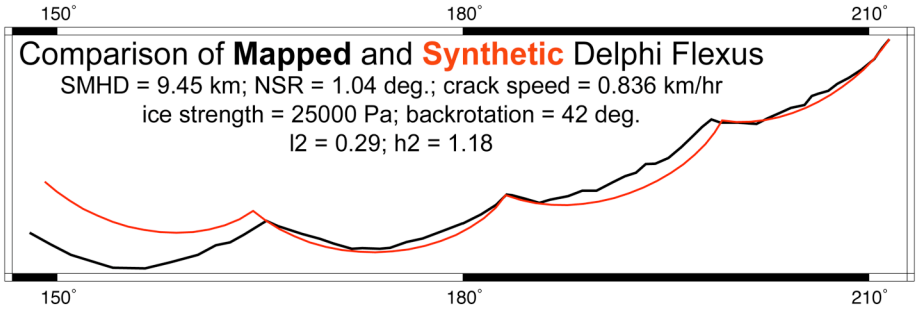

Figure 4.2a: SMHD and input parameters for the synthetic lineament (in **red**) which most resembles the planform of Delphi Flexus as mapped (in **black**). Found using the Neighborhood Algorithm.

Figure 4.2b: SMHD and input parameters for the synthetic lineament (in **red**) which most resembles the planform of Cilicia Flexus as mapped (in **black**). Found using the Neighborhood Algorithm. Best fit parameters for Delphi and Cilicia Flexus are strikingly similar. Love numbers correspond to a single layer 20 km thick elastic ice shell over an 80 km deep ocean.

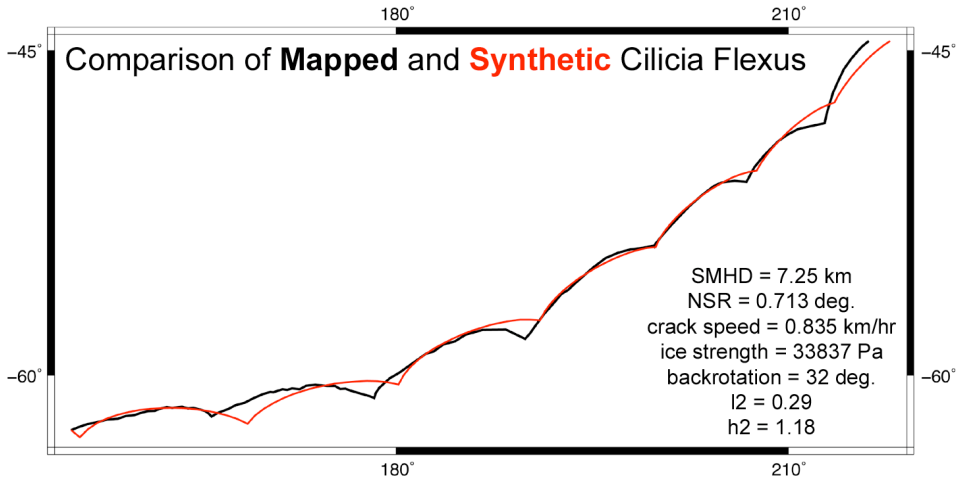

5. Computer Assisted Stratigraphic Sorting

The Law of Superposition is one of the founding principles of modern geology laid down by Nicolaus Steno in the 17th century. Stated plainly: layers of rock are arranged in a time sequence, with the oldest on the bottom and the youngest on the top, unless later processes disturb this arrangement. Europa's young surface lacks a large number of craters and the well understood impactor population which in combination have been so useful in determining relative and absolute surface ages on the terrestrial planets using superposition.

Fortunately Europa's surface geology has provided us with an enormous selection of surface units and structures having a vast number of cross-cutting relationships, in the form of the ubiquitous lineaments that cover the majority of the surface. Linear features can have an almost unlimited number of intersections, while allowing plenty of space on the surface for other linear features. In principle at least, the cross-cutting relationships of the lineaments provide us with a rich source of information about the moon's history. This potential dataset has yet to be substantially tapped.

Because the amount of information contained in the lineament intersections is so large, extracting it manually is impractical. Even in a small area, one may find hundreds of lineaments, having thousands of intersections. Disentangling them by hand is labor intensive and error prone. Additionally, it is important to be able to distill and display the most scientifically useful information out of this large pool of data. To perform these tasks in a repeatable way, such that human subjective bias is minimized and the limitations of the information extracted can be quantified, an algorithmic approach implemented by a computer is required. The approach I implement is generally applicable to any set of features that have clear superposition relationships.

5.1 From Map to Graph

In order to manipulate the network of features and intersections algorithmically, the spacecraft images must be converted into a data structure representing the relevant information. The natural choice in this case is a construct known in mathematics as a *directed graph* or *digraph*. A digraph can be visualized as a set of points connected by unidirectional arrows. Each point is known as a *node* or *vertex* and each arrow is known as an *edge*. Nodes and edges can both have data associated with them.

When converting the map to a digraph, each node represents a mapped feature, and each edge represents a crosscutting relationship. If there is an edge from node A to node B, this means that feature A intersects feature B, and that at their intersection A appears to be on top of B. In a simplified world, where each feature forms instantaneously at a time unique from all other features, and is never active again, the graph representing the features and their crosscutting relationships would have a particular structure: if one were to traverse such a graph, traveling from node to node along the unidirectional edges, once a particular node had been visited, and left behind, it would never again be encountered. This kind of graph is known as a *directed acyclic graph* or DAG (see Fig. 5.1).

DAGs have the property that they can be *topologically sorted*. That is, for any DAG there exists an ordering (usually many orderings) of the nodes such that all of the edges in the graph only point one way along the ordering. If one were to traverse a graph so ordered, travel is only possible in one direction in the list. In the graphs I construct representing features on Europa's surface the directed edges represent temporal relationships based on superposition. Thus, when the graphs are topologically sorted, the features are actually being ordered temporally, consistent with their crosscutting relationships with each other.

I introduce a further refinement to the concept of a topologic sort which I term a *stratigraphic sort.* Whereas any particular topologic sort is only one of potentially many self-consistent orderings, a stratigraphic sort seeks to convey the range of possible topologic sorts, allowing us to quantify how unique (and thus how meaningful) the ordering we obtain is. Performing a stratigraphic sort on a DAG consists of the following procedure:

1.) Set N=1
2.) Identify all nodes which only have edges *emanating from* them (representing features which are stratigraphically "on top" of everything they cross).
3.) Remove these nodes from the graph, and tag them with the number N.
4.) Repeat steps 1 and 2, incrementing N each time, until there are no longer any nodes in the graph.
5.) Re-constitute the original graph and additionally tag each node with the value M, which is defined to be the smallest value N associated with any of that node's descendants (those other nodes "downstream" of the node in question, following the directed edges).

Thus, the pair of values (N,M) associated with each node define the uppermost and bottommost layer in the stratigraphic stack which each node could potentially belong to. Each layer in the stack is composed of the set of all lineaments which are stratigraphically indistinguishable from each other based on their crosscutting relationships. The greater the value of (M-N) for a particular feature, the less well constrained its stratigraphic location is.

If it is hypothesized that lineaments at similar locations in the stratigraphic sequence ought to have formed in similar stress environments, and thus have similar orientations, then the stratigraphic sort can be further refined by using information we have about the lineaments' orientations. By comparing the orientation of each lineament with an ambiguous stratigraphic location, to the average orientation of the lineaments in each of the possible stratigraphic layers the ambiguous lineament could belong to, it may be possible to narrow down the number of plausible layers, excluding those which are too far from being parallel to our ambiguous lineament.

This kind of refinement will only work so long as the timescale on which lineaments form is significantly shorter than the timescale on which stress directions change. It should actually be possible to see whether this is the case or not, by looking at the original results of our sort – if there are many layers in the stratigraphy which have a very small number of members then the timescale for re-orientation of the failure direction is shorter than timescale on which lineaments form. If there are many layers which have multiple members with similar orientations then it is more likely that lineament formation happens on a short timescale relative to the change in failure direction, and the refinement of the stratigraphic sort based on orientation would appear to be justified.

5.2 The Implications of Lineament Reactivation

Early applications of the stratigraphic sorting method to the E15REGMAP01 area on Europa indicate that the idealization made in the previous section requiring lineaments to form instantly, at unique times, and never reactive, is unrealistic. In fact the graphs which represent the mapped lineaments and their intersections are *not* DAGs – they contain cycles, in which lineament A overlies B, B overlies C, and C (or one of its descendants) ultimately overlies A. This is an interesting observation in its own right – it implies that lineaments are either forming contemporaneously, but with different orientations (allowing them to intersect), or that sections of old lineaments are being reactivated and reversing their crosscutting relationships with younger lineaments that intersect them.

Initially I thought it was likely that this was the result of using ambiguous intersections in which it was difficult to conclusively say which feature was on top. To try and avoid this problem, each intersection was given a *confidence* value between 0 and 1, with 0 representing a completely ambiguous crosscutting relationship, and 1 representing a completely obvious crosscutting relationship. The dataset input to the stratigraphic sorting algorithm was then limited to include only intersections exceeding a certain minimum threshold confidence. The threshold value was then increased until a DAG resulted from the conversion of the map to a graph. Surprisingly, the threshold value at which this finally happened was 0.9, meaning that there still existed cycles even when only very clear crosscutting relationships were involved – i.e. the cycles were real, and not just the result of bad input data. If the ice is failing in tension, the failure direction should be well defined at any given time, and the simplest explanation of these cycles would seem to be the reactivation of old fractures.

A stack of lineaments which has cycles in the graph representing it cannot be stratigraphically sorted, but if reactivation is relatively infrequent, the cycles can be removed without losing too much of the original information by finding a small set of edges which when removed from the graph makes it acyclic. If reactivation further occurs along continuous segments of the lineaments, such that several adjacent intersections are overprinted simultaneously, those lineament segments which are most likely to have experienced reactivation can potentially be identified, along with the point in the stratigraphy at which the reactivation occurred. To some degree it is also possible by analyzing the structure of the graph whether or not it is valid to assume that reactivation is uncommon.

To allow the sorting technique to deal with lineament reactivation I need to introduce a few more concepts (and terminology) from graph theory. Each node has some number of edges coming in, and some number going out. These numbers are known as the node's *in degree* (D_{in}) and *out degree* (D_{out}) respectively. The sum of these numbers is simply the node's *degree*. A node's *net in degree* is (D_{in}-D_{out}), and its *net out degree* is (D_{out}-D_{in}). A *source node* is a node with D_{in}=0, a *sink node* is a node with D_{out}=0. Edges frequently have numerical values associated with them known as *weights*. In this model, the confidence value associated with each intersection is the weight associated with its corresponding edge. Edges with larger weights are more important to us because we are more sure of

the information which they represent. They are a way of making the very discrete graph representation more continuous. A node's *weighted in degree* and *weighted out degree* are the sums of the weights of the incoming and outgoing edges, respectively

The problem of removing the *optimal* set of edges (defined as the set of edges with the minimum sum of weights) from an arbitrary digraph to make it into a DAG takes O(|E|!) time (where |E| is the size of the set of edges E), and is thus computationally intractable for an arbitrary digraph with even a modest number of edges. To quickly and surely render an arbitrary digraph acyclic, one can order the nodes in a list, and then remove either all the edges which go up or down the list. This ensures that you always keep at least half of the original edges. Luckily there is good reason to believe that the graphs we generate will not be arbitrary.

If the hypothesis that lineament reactivation is relatively rare is correct, then the graphs are expected to be close to acyclic, as mapped, since for the most part the intersections we have mapped should be telling a well ordered stratigraphic story. If an *a priori* quasi-temporal ordering of the nodes could be found, it would have many more edges going one direction than the other along the list. It turns out that ordering the nodes by their *net weighted out degree* does just this, since those lineaments which formed longer ago tend to have more intersections in which they are on the bottom. An even better measure would be net weighted out degree per unit length, since one would expect that the number of intersections an individual lineament has, to scale linearly with its length.

If the hypothesis that reactivation is rare is incorrect, then ordering the nodes this way will not create a graph with many more edges going one direction than the other. Early work on the E15REGMAP01 region has produced highly asymmetric graphs, so the hypothesis appears to be correct, and there is hope that this technique may be productive. In fact, it may be possible to infer approximately how frequent reactivation has been in a region based on how cyclic the graphs generated there are.

5.3 Breaking the Vicious Cycles

Once the nodes have been ordered according to their net weighted out degree per unit (lineament) length, the vast majority of the edges will be going in the direction from generally newer features to generally older features, but since our graph is not acyclic, there will be at least a few which are going the other way. These are called *back edges*. The simplest way to enforce a DAG is to remove all the back edges, but they may or may not actually be involved in cycles, and so by simply removing them without checking, we risk losing information unnecessarily.

To determine which nodes and edges are actually involved in cycles it is useful to note that in order to be involved in a cycle, a node must have both D_{in} and $D_{out}>0$, so neither source nor sink nodes can ever be involved in a cycle. A temporary copy of the graph is made, and all source and sink nodes as well as all the edges connected to them are removed since none of them are to blame for the cycles. The smaller resulting graph may also contain source and sink nodes, and similarly, none of them could have been involved in cycles either. We can repeat this process of source and sink node removal until we are left with a graph that contains no source and sink nodes. The remaining nodes and edges are those which could be involved in cycles.

At this point, it will be useful to note which of the remaining nodes have the most back edges coming from them – these are the most likely features to have experienced reactivation. If the intersections represented by back edges in the original ordered graph are highlighted on the map sometimes they are found to be grouped preferentially along contiguous portions of the features called out above as being the most likely candidates for reactivation. Such lineaments can be broken into two sections (the reactivated section, and the quiescent section), based on where we see the back edge intersections, the two segments treated as separate features, and used to create a new ordered graph. If the lineament has been broken in the correct location, the new graph should have fewer back edges and fewer cycles than the original, and the two segments of the split lineament should sort to different locations in the stratigraphy, corresponding to the times of original formation and reactivation. If the lineament has been split incorrectly, the number of back edges and cycles will not change significantly, and the two lineament segments ought to ultimately sort to a similar location in the stratigraphy.

If after splitting all clear candidates for reactivation, the graph is still not acyclic, edges or nodes will have to be removed resulting in the loss of some of the originally mapped information. If the set of nodes and edges in the portion of the graph which has no source or sink nodes is small enough, we can perform an exhaustive search for the optimal feedback edge set. An exhaustive search will still take O(|E|!) time. If the search is restricted to only considering back edges for removal this may be

acceptable, otherwise a heuristic approach will be needed. One approach is a greedy algorithm which tries removing each of the remaining nodes one at a time, to see which one creates the most new source and sink nodes (which can again be iteratively removed until a new set of nodes and edges involved in cycles is reached). That node which resulted in the best ratio of new source and sink nodes to information lost (the sum of the weights of all of the edges which were removed), is then added to the list of features which must be ultimately removed. This process is repeated until we finally have an acyclic graph, at which point the stratigraphic sort can be performed.

5.4 Questions Stratigraphic Sorting may Answer

After having done the above, there should be at least tentative answers to the following questions:

1.) Which parts of what lineaments are most likely to have reactivated?
2.) At what point in the stratigraphic history did those reactivations occur?
3.) How much reactivation has the region in general has been subject to? (as indicated by how cyclic the original graph is)
4.) How has the orientation of fracture formation changed through time?
5.) What are the relative rates of lineament formation and stress re-orientation? (based on the number of similarly oriented lineaments in each layer, and how much orientation changes between layers).
6.) What kind of stress environment causes reactivation? (i.e. how are the stresses oriented relative to lineaments when they reactivate)

5.5 Validating the Stratigraphic Sorting Method

However, before we can be confident in the results that the stratigraphic sorting method yields, its performance will need to be tested on synthetic datasets whose histories we know. This will allow investigation of its limitations as input datasets become more and more ambiguous. Several metrics of performance can be used:

1.) fraction of ordering information recovered unambiguously
2.) frequency with which features are unambiguously ordered *incorrectly*
3.) frequency with which lineaments are correctly (and incorrectly) identified as having undergone reactivation
4.) frequency with which lineaments correctly identified as having undergone reactivation can be correctly split into active and quiescent segments
5.) recovery of time variability of failure orientation

In addition, it will be important to see how the above performance metrics respond to changes in the input dataset, such as:

1.) frequency of lineament reactivation
2.) distribution of lengths of segments which reactivate
3.) distribution of intersection confidence values
4.) correlation between reactivation and intersection confidence values
5.) length to spacing ratio of mapped lineaments (influences frequency of intersection)
6.) variation in rate of lineament formation relative to rate of change of failure orientation

Separately, I will investigate the correlation between reactivation frequency and the proportion of nodes and edges involved in cycles, in order to be able to assess possible study sites for use with the method.

Ultimately, synthetic test cases will be designed which are statistically as similar as possible to actual regions of study on Europa, with similar distributions of confidence values, similar length/frequency distribution in the mapped features, similar distributions of lineament orientations, and reactivation at a level which results in a similar graph structure to the region mapped. The results from those test cases should indicate how trustworthy the results from the actual study sites really are. These investigations of various study sites will also inform us as to how similar the lineament formation histories of different mapped regions are, even if we cannot directly infer what those histories are.

5.6 Potential Study Sites

The stratigraphic sorting method described above is broadly applicable with minor alterations to any set of mapped features which have clear crosscutting relationships. On Europa I plan to apply the technique to regional or higher resolution image mosaics, including the two north to south REGMAP mosaics at 80° and 220° longitude, and the areas surrounding Conamara Chaos and Agenor Linea. It may also be productive to apply it to the global scale lineaments discussed in section 3 above, as previous work has suggested that the apparent crosscutting relationships between global lineaments

requires more than 180° of shell rotation to account for, given the best fits of the global lineaments to NSR stresses (Figueredo and Greeley 2000). The method has already been used with some success to infer the order of formation of grooved terrain on Ganymede (Martin et al., 2006). Other icy satellites such as Enceladus in the Saturnian system are also prime candidates for study.

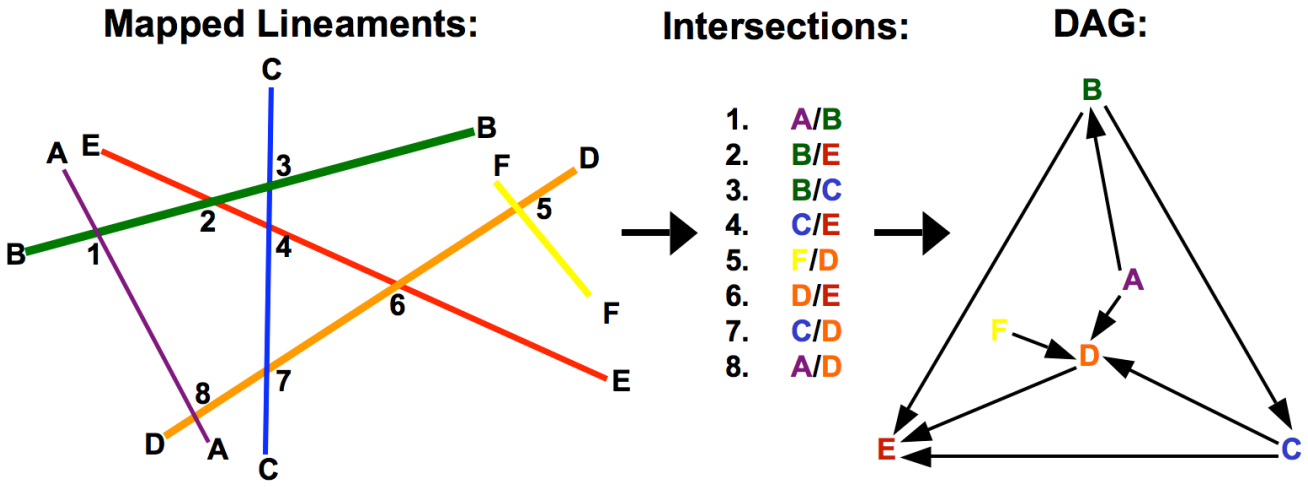

Figure 5.1: Mapped lineaments A-E each have a unique time of formation. When their intersections are used to construct a graph, it is acyclic.

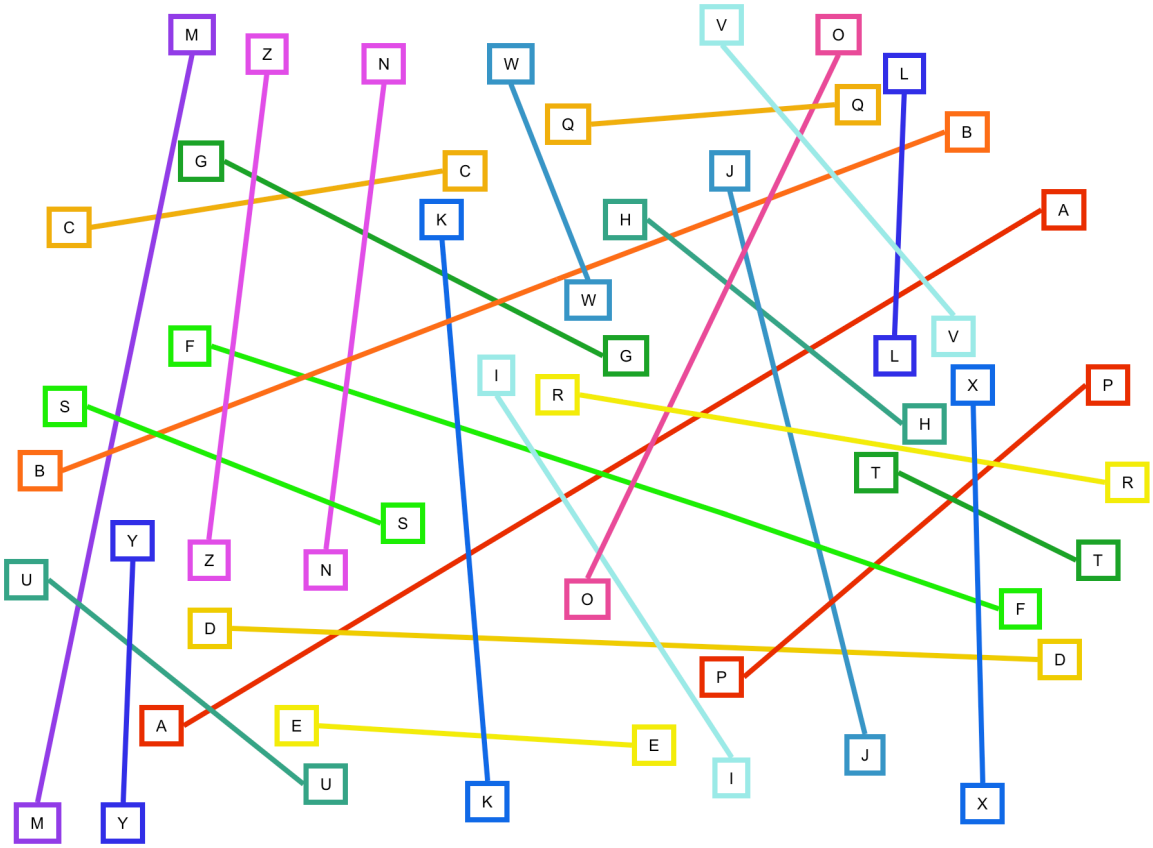

Figure 5.2: This map of 26 synthetic lineaments formed in a tensile stress field which was rotating clockwise with time. The lineaments originally formed in alphabetical order (as labeled here). Reactivation occurred along B at the time of P's formation, and along F at the time of R's formation. This map is represented by the graph and sort in Fig. 5.3.

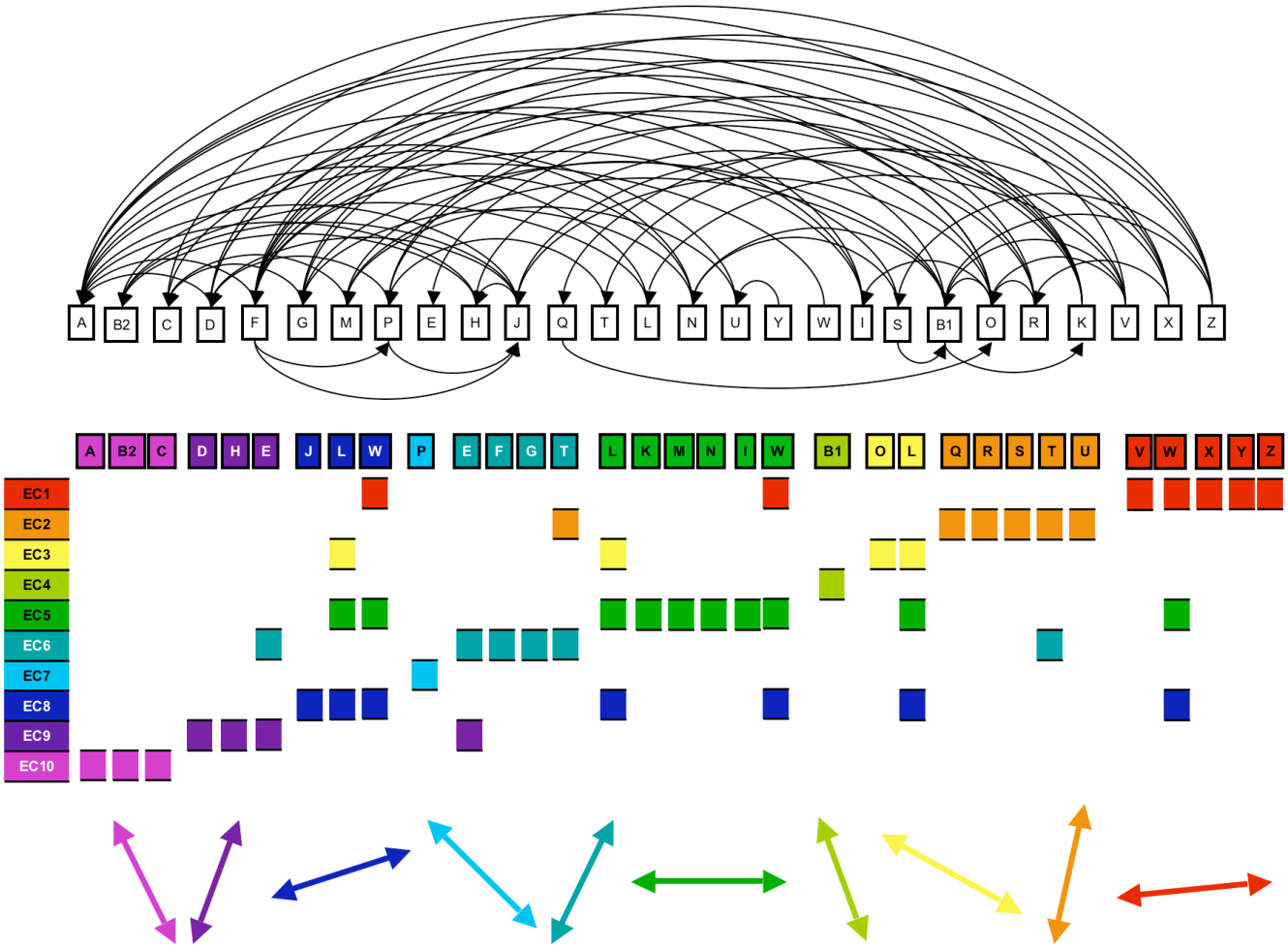

Figure 5.3: The highly asymmetric graph at the top of the figure is acyclic. It represents the crosscutting relationships between the lineaments pictured in the map in Fig. 5.2. The lineament B has been split into two separate features, B1 and B2, as the result of an initial sort in which it was found to be the source of several back edges. The lineament was split according to the geographic locations of the intersections which were represented by back edges. The segment which reactivated, B1, has been successfully placed in the stratigraphy at the time of reactivation.

In the middle, each row (and color) corresponds to one stratigraphically indistinguishable equivalency class (EC). Each lineament has a column for each EC to which it may belong, as constrained by both its crosscutting relationships and its orientation.

The arrows at the bottom show the average orientation of the lineaments in each EC which are constrained to belong to only that EC. They reflect a clockwise rotation of the tensile failure direction with time.

6. Looking Forward

With the techniques described above and the new viscoelastic ice shell model, it should be possible to extract new information from the Galileo dataset, and to help inform Cassini's investigations of Saturn's moons. Icy satellites have consistently demonstrated a surprising degree of dynamism and complexity for their diminutive size, and they continue to present new challenges whenever one takes the time to look a little closer.

Measuring the time variability of the rate of global lineament formation may provide information about changes in the ice shell or its rotation rate. For instance, if the rate of global lineament formation due to NSR stresses were to steadily increase, and then decrease rapidly toward the end of the relative timeline, before being supplanted by more wavy and cycloidal lineament formation, we might hypothesize that the rate of ice shell rotation had slowed over time, increasing the NSR forcing period, before finally becoming tidally locked – perhaps as a result of a mass anomaly within the shell, similar to those which have been detected on Ganymede (Anderson et al., 2004). As the forcing period first exceeds the

relaxation time of the warm lower portion of the ice shell, NSR stresses would be concentrated in the cold upper portion of the shell, leading to an increased rate of lineament formation. Then as the shell further slowed its rotation, the forcing period would eventually exceed the relaxation time of the upper shell, leading to a dramatic reduction in NSR stresses, allowing diurnal stresses to become dominant.

Characterizing the topologic properties of the graphs which result from mapping crosscutting relationships between lineaments on different parts of Europa's surface gives us a new way to compare regions. It may turn out that different regions have different relative rates of lineament formation and stress reorientation. Or it may be that regions previously thought of as dissimilar actually share similar rates of reactivation and stress reorientation.

Allowing the ice shell to reorient arbitrarily in an effort to reproduce the cycloidal lineaments in the equatorial regions may hint at the history of Europa's ice shell reorientations, if any, which may in turn give us insight into the frequency and magnitude of mass redistribution within the shell.

All of these investigations will help to shape and enrich our understanding of the tidally driven dynamics within Europa and other icy moons. Tides and the processes they drive on icy satellites seem analogous to radiogenic heating and plate tectonics on Earth, resurfacing, recycling, and potentially ensuring a continuous flow of heat and chemical energy which, if the tenacity and patience of terrestrial organisms is any indication, ought to be sufficient to support life in these deep, dark, unseen oceans.

7. References

Anderson, J.D., G. Schubert, R.A. Jacobson, E.L. Lau, W.B. Moore, J.L. Palguta, Discovery of Mass Anomalies on Ganymede, *Science, 305,* 989-991, 2004.

Bierhaus E.B., Chapman C.R., Merline W.J., Brooks S.M., Asphaug E., Pwyll Secondaries and Other Small Craters on Europa, *Icarus, 153*, 264-276, 2001.

Cassen, P.M., S.J. Peale, and R.T. Reynolds, Structure and thermal evolution of the Galilean satellites, in Satellites of Jupiter (D. Morrison, ed.), University of Arizona Press, Tucson, pp. 93-128, 1982.

Cormen, T.H., C.E. Leiserson, R.L. Rivest, and C. Stein. Introduction to Algorithms 2nd Ed., MIT Press and McGraw-Hill. pp. 549–552, 2001.

Crawford, Z.A. and R.T. Pappalardo, Evidence for episodic formation of Europa's global lineaments via non-synchronous rotation, LPSC XXXVII, abstract #2264, 2006.

Figueredo, P.H. and R. Greeley, Geologic mapping of the northern leading hemisphere of Europa from Galileo solid-state imaging data, *JGR Planets, 105,* 22629-22646, 2000.

Geissler, P.E., R. Greenberg, G. Hoppa, P. Helfenstein, A. McEwen, R.T. Pappalardo, R. Tufts, M. Ockert-Bell, R. Sullivan, R. Greeley, M. Belton, T. Denk, B. Clark, J. Burns, and J. Veverka, Evidence for Non-synchronous Rotation of Europa, *Nature*, *391*, 368-370, 1998.

Greeley, R., C.F. Chyba, J.W. Head III, T.B. McCord, W.B. McKinnon, R.T. Pappalardo, P. Figueredo in: Jupiter: The Planet, Satellites & Magnetosphere (F. Bagenal et al., eds.), Cambridge University Press, pp. 329-362, 2004.

Greenberg, R., P.E. Geissler, G. Hoppa, B.R. Tufts, D.D. Durda, R.T. Pappalardo, J.W. Head, R. Greeley, R. Sullivan, and M.H. Carr, Tectonic processes on Europa: Tidal stresses, mechanical response, and visible features, *Icarus*, *135*, 64-78, 1998.

Gromov, M. Metric Structures for Riemannian and non-Riemannian Spaces, Birkhäuser,1999.

Helfenstein, P. and E.M. Parmentier, Patterns of fracture and tidal stresses due to nonsynchronous rotation: Implications for fracturing on Europa, *Icarus*, *61*, 175-184, 1985.

Hoppa, G.V., *Europa: Effects of Rotation and Tides on Tectonic Processes*, Ph.D. Thesis, University of Arizona, 1998.

Hoppa, G.V., B.R. Tufts, R. Greenberg, P. Geissler, Formation of Cycloidal Feattures on Europa, *Science, 285*, 1999.

Hoppa G.V. , R. Greenberg, P. Geissler, B.R. Tufts, J. Plassmann, D.D. Durda, Rotation of Europa: Constraints from Terminator Positions, *Icarus, 137,* 341-347, 1999.

Hussman H. and T. Spohn, Thermal-orbital evolution of Io and Europa, *Icarus, 171,* 391-410, 2004.

Kivelson, M.G., K.K. Khurana, C.T. Russell, M. Volwerk, R.J. Walker, and C. Zimmer, Galileo magnetometer measurements: A stronger case for a subsurface ocean at Europa, Science, 289, 1340-1343, 2000.

Leith, A.C., and W.B. McKinnon, Is there evidence for polar wander on Europa?, *Icarus*, *120*, 387-398, 1996.

Martin, E.S., G.C. Collins, Z.A. Crawford, R.T. Pappalardo, Computer assisted time sequence sorting of grooves in eastern

Mysia Sulci, Ganymede, LPSC XXXVII, abstract #1204, 2006.

McEwen, A.S., Tidal reorientation and the fracturing of Jupiter's moon Europa, *Nature*, *321*, 49-51, 1986.

McEwen, A.S., L.P. Keszthelyi, R. Lopes, P.M. Schenk, J.R. Spencer, The Lithosphere and Surface of Io in: Jupiter: The Planet, Satellites & Magnetosphere (F. Bagenal et al., eds.), Cambridge University Press, pp. 307-328, 2004.

Moore, W.B. and G. Schubert, The tidal response of Europa, *Icarus, 147*, 317-319, 2000.

Mullen, M.E., *Viscoelastic Surface Stresses on Europa*, Honors Thesis, University of Colorado, 2006.

Ojakangas, G.W. and D.J. Stevenson, Thermal state of an ice shell on Europa, *Icarus*, *81*, 220-241, 1989a.

Sambridge, M., Geophysical Inversion with a Neighbourhood Algorithm I: Searching a parameter space, *Geophysical Journal International*, *138*, 479-494, 1999a.

Sambridge, M., Geophysical Inversion with a Neighbourhood Algorithm II: Appraising the ensemble, *Geophysical Journal International*, *138*, 727-746, 1999b.

Sarid A.R., Greenberg R., Hoppa G.V., Hurford T.A., Tufts B.R., Geissler P., Polar Wander and Surface Convergence of Europa's Ice Shell: Evidence from a Survey of Strike-Slip Displacement, *Icarus, 158,* 24-41, 2002.

Showman, A. P., D. J. Stevenson, and R. Malhotra, Coupled orbital and thermal evolution of Ganymede, *Icarus*, *129*, 367-383, 1997.

Wahr, J., A.C. Barr, G.C. Collins, Z.A. Crawford, M.E. Mullen, R.T. Pappalardo, M.M. Stempel, Modeling the tidally induced viscoelastic surface stresses of icy satellites: an application of potential theory, in preparation.

Zahnle K., P. Schenk, H. Levison, L. Dones, Cratering rates in the outer Solar System *Icarus*, *163*, 263-289, 2003.